International Journal of Bio-Inorganic Hybrid Nanomaterial

Room Temperature Ferromagnetism in Cobalt Doped ZnO Nanoparticles

Mirabdullah Seyed Sadjai[*], Abdolazim Azimi, Nasibeh Mollahasani, Faranak Asgari

Department of Chemistry, Sciences and Research Branch, Islamic Azad University, Tehran, Iran

ABSTRACT

In this work we report synthesis and magnetic characterization of cobalt doped ZnO nanoparticles (with different percent of doped cobalt oxide). Synthesis of the materials was carried out at room temperature by polyacrylamide-gel method, using zink sulfate and cobalt nitrate as source materials, acrylamide as monomer and N,N-methylene bisacrylamide as a lattice reagent. Characterization of the samples were performed using XRD, SEM, TEM, UV and photoluminescence (PL) studies. The X-ray diffraction patterns obtained showed formation of wurtzite ZnO structure with no secondary Co phases. The EDS measurements were employed to investigate the composition of the samples and showed the presence of Zn and cobalt elements detected. The optical absorption spectra showed internal d-d transitions related to Co^{2+} incorporated on the Zn lattice site of ZnO structure. The red-shift of the band-gap edge has been attributed to a merging of donor and conduction bands due to the Co doping. The magnetic behavior of prepared cobalt doped samples was finally investigated at room temperature using vibrating sample magnetometer (VSM). The results show that, the Co doped ZnO. Nanoparticles with 2at% CoO is ferromacnetic at RT. This magnetic property is greatly suppressed and replaced by a paramagnetism behavior at higher doping levels.

Keyword: cobalt doped ZnO; photoluminescence; ferromagnetism; diluted magnetic semiconductor; spintronics.

1. INTRODUCTION

In the field of spintronics, studying of semiconductors with ferromagnetically polarizable carriers at room temperature (RT) is a very interesting subject to study. In these kinds of materials, the spin and charge of the carriers can be coupled separately with an external magnetic field. While, electrons carry both charge and spin and processing of the information in conventional electronic devices is based only on the charge of the electrons while spin electronics or spintronics, uses the spin of

(*) Corresponding Author - e-mail: Msadjadi@srbiau.ac.ir

electrons, as well as their charge, to process information. By using this type of material it has been possible to integrate electronics, magnetism and optical functionalities in a single material, leading to a low cost, high-speed, and small size controlling devices operating at very low power [1-4]. Today, due to the revolution in our understanding in generating, manipulating and detecting *spin-polarized* electrical current, making entirely new classes of spin-based sensor, memory and logic devices have been possible [5].

To this end, several experimental groups have been attempted for preparation of the magnetic semiconductors in the various host semiconductor materials such as ZnO, TiO_2, and In_2O_3, by doping with 3d transition metals [6-7] after theoretical prediction of such materials, "so-called diluted magnetic semiconductor (DMS)," operational at RT by Dietl et al. [8]. For most of the experimental results obtained, doubts arose about the real origin of ferromagnetism (FM). For some cases, it was demonstrated that the ferromagnetism is due to segregation of metallic clusters while in some systems it occurs because of the transition-metal elements in different valence states. Recently, it was reported that the host material itself without any magnetic element doping becomes magnetic when the size of the crystallites is in nanometers size [9-12].

To receive a good understanding of origin of ferromagnetism in DMS, investigation on the ferromagnetic and optical properties of highly transparent and interinsically n-type conducting zink oxide doped with the 3d transition metal Co (ZnO with different percent of cobalt oxide) seems still interesting and promising for the emerging field of spintronics. In this work, synthesis and opticalmagnetic characterization of cobalt doped ZnO nanoparticles.

2. EXPERIMENTAL

2.1. Materials
Acrylamide (AM) (99.0%), N,N-methylenebisacry- lamide (MBAM) (99.0%), ammonium persulphate (APS), $ZnSO_4.7H_2O$ (99.5%), $Co(CH_3COO)_2.H_2O$ (99.5%) were received from merk chemical company and used without further purification. Double distilled water was used for the preparation of any solution in this study.

2.2. Nanoparticle preparations
Poly (acrylamide) hydrogels were prepared by mixing 5 g of AM dissolved in 3ml of distilled water at the presence of a cross-linker (MBAM) and initiating system (AMP). The mass ratio between monomer and lattice reagent was 5:1 and the polymerization was performed in 25 mL beakers at 800C temperature within 1h of reaction time. For preparation of ZnO-CoO nanoparticales, a mixture of acrylamide as monomer and N,N-methylenebisacrylamide as lattice reagent was added to the aqueous solution of Zn^{2+} and Co^{2+} prepared by dissolving $ZnSO_4.7H2O$ and $Co(CH_3COO)_2.H_2O$ in desired proportions in water. The mixtures obtained were then heated to dissolve completely the solutes and polymerized after addition of ammonium persulfate within 1h of reaction time at 80°C. The wet gels obtained were finally dried for 2h at 100°C to produce dried gels and calcined in the furnace at 500°C temperatures.

2.3. Characterization
Powder X-ray diffraction (XRD) patterns were recorded on a Seisert Argon 3003 PTC diffractometer using Cu k_α radiation (λ = 0.15406 nm). UV-visible spectra were recorded on an UV-visible Hitachi spectrophotometer model U-2101 PC. The solution forms of the samples were prepared by suspending a small amount of powder in ethanol. Scanning Electron Microscopy (SEM) images of the samples were obtained using a LEOVP1200 electron microscope. The samples were rinsed with distilled water, dried and coated with a thin layer of gold by evaporation at vacuum to form conducting film. The magnetic properties of the samples were measured by vibrating sample magnetometer (VSM) using on a physical property measure system (Quantum Design PPMS-9).

Sadjadi MS et al

Int. J. Bio-Inorg. Hybd. Nanomat., Vol. 1, No. 2 (2012), 123-130

3. RESULTS AND DISCUSSION

3.1. Structural characterization

Figure 1 shows XRD patterns of ZnO and as pre-pared samples containing 2, 5 and 10% of cobalt oxide. All diffraction peaks corresponding to the (100), (002), (101), (102), (110), (103), (112) and 201) planes are sharp and strong, suggesting that the products are highly crystallized, and all the visible diffraction peaks in this pattern can be well indexed to the wurtzite ZnO structure (hexagonal crystal system, P63 mc space group, JCPDS card No. 36-1451). No other diffraction peaks con-cerning to the presence of cobalt oxides in the XRD pattern indicates the presence of no additional crystalline structures in the prepared samples. This observation implies incorporation of the Co ions in the lattice site of ZnO structure by means of Zn substitution rather than interstitial ones. It is report-ed that, the substitution of Co^{2+} in ZnO lattice matrix [13,14] induce an obvious shift of (002) peak position to the smaller angles in Co-doped ZnO nanorods due to the smaller radius of Co^{2+} ions (0.58 A) than that of the Zn^{2+} ions (0.60 A). However, in our case, the peak shift in XRD pattern for Co doped ZnO nanocrystals is indiscernible, due to the limited resolution of the usual XRD measure-ment. Similar results about indiscernible peak shift in XRD patterns were also reported for Co-doped
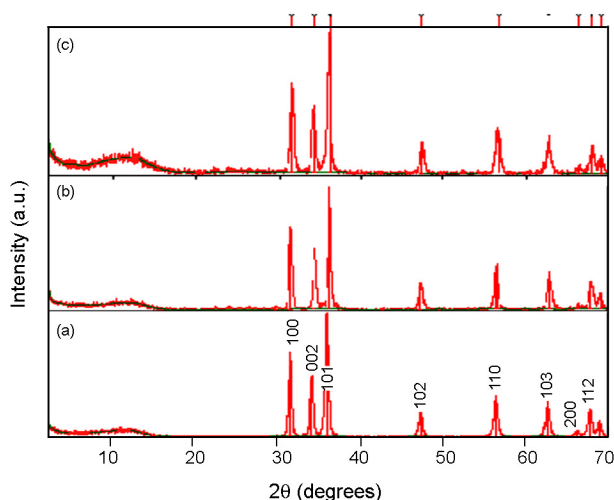
ZnO nanoparticles by some other reports [15-18]. In this diffraction pattern, we selected the peak at 2θ values of 25.9° corresponding to (002) miller plane to calculate the average crystalline size, as (002) peak is an isolated sharp peak with relatively high intensity, by using Scherrer's formula $\beta \cos \theta = (K\lambda/D)$, where β is the full width at half maximum (FWHM) in radians, D is the average crystallite size, λ is the x-ray wavelength (CuK λ = 0.154 nm), θ is the Bragg diffraction angle and K is a correction factor which is taken as 1. The calculated crystallite sizes (D) of the prepared samples were estimated to be 16.2, 20.80, 20.92 and 20.38 nm.

3.2. FTIR studies

Figure 2 Shows FT-IR spectra of cobalt doped ZnO samples obtained after calcination at 500°C. No organic network trace has been observed in the spectra. The characteristic bond at 3450 and 1636 cm^{-1} are assigned to the existence of hydroxy-yl groups on the surface of the samples in all the cases. The two broad peaks observed at 1130 and 1228 cm^{-1} belonged to internal and external asym-metric Zn-O and Co-O stretching modes. The peaks at 458 and 531 cm^{-1} are characteristic of the Zn-O and Co-O metal oxide bands and can be assigned to the asymmetric stretching mode of the tetrahedral
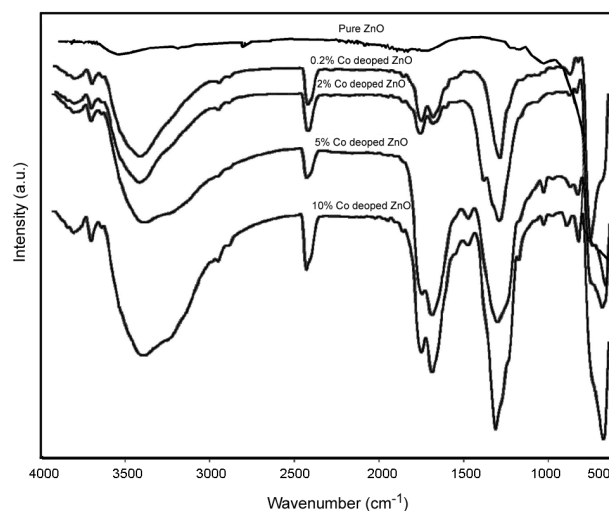

Figure 1: *XRD patterns of as prepared ZnO samples doped with 2.0 (a); 5.0 (b) and 10 at% (c) cobalt oxide.*

Figure 2: *FTIR spectra of (a) pure ZnO, and cobalt doped samples with: (b) 0.2; (c) 2.0; (d) 5.0 and (e) 10 at% cobalt oxide.*
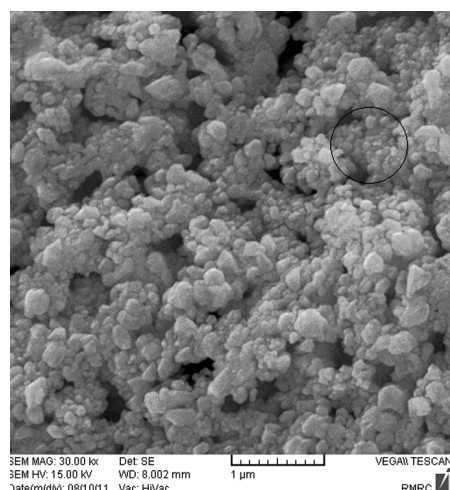
Figure 3: *SEM image of Cobalt doped ZnO nanoparticles containing 2 at % cobalt oxide.*

ZO4 groups present in the wurtzite ZnO structure [19].

3.3. SEM images
Figure 3 Shows SEM image of homogeneous distribution of 2at% cobalt doped ZnO nanoparticles.

3.4. EDAX analysis
Figure 4 and Table 1 give ESD analysis data obtained for ZnO samples doped with 2 at% cobalt oxide as an example. These results confirm coexistence of ZnO and cobalt oxide in the prepared samples.

3.5. Magnetic characterization
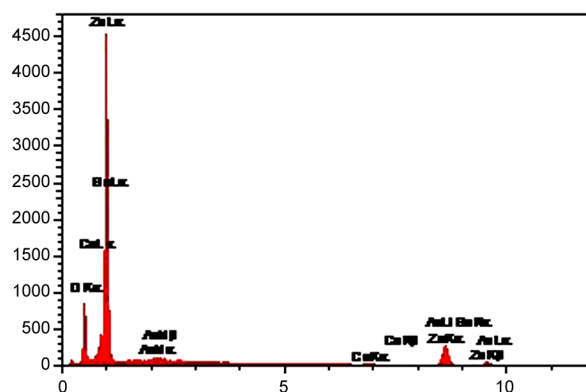Figure 5 (a,b,c) shows the Dc magnetic-field-

Figure 4: *X-ray dispersive (EDAX) result for ZnO samples containing 2 at % cobalt oxide.*

dependent magnetization curves M(H) for the cobalt doped zink oxide nanoparicles ($Zn_{1-x}Co_xO$, (x=2.0, 5.0 and 10), at room temperature, using vibrating sample magnetometer. Figure 4a shows that, the saturation magnetization M as a function of the magnetic field H has "S"-shaped behavior at room temperature. It is clear that the S-shaped curves with a finite low value of coercivity (Hc) and remanence (Mr) at room temperature (Hc = 0.0 KOe; Mr = 0.0 emu/mole, indicates, that Co doped ZnO nanoparticle with 2at% CoO is ferromacnetic at RT. The saturation magnetizations (Ms = 4.04 emu/g) for this composite is approximately the same value reported for 3 w% Co doped ZnO after 2 h milled sample [20] which, can be due to the electrons which induce more effective ferromagnetic couplings between doped Co^{2+} ions But, this magnetic behavior of cobalt doped ZnO is

Table 1: *EDAX ZAF quantification (standardless) element normalized for the sample containing 2 at% cobalt oxide.*

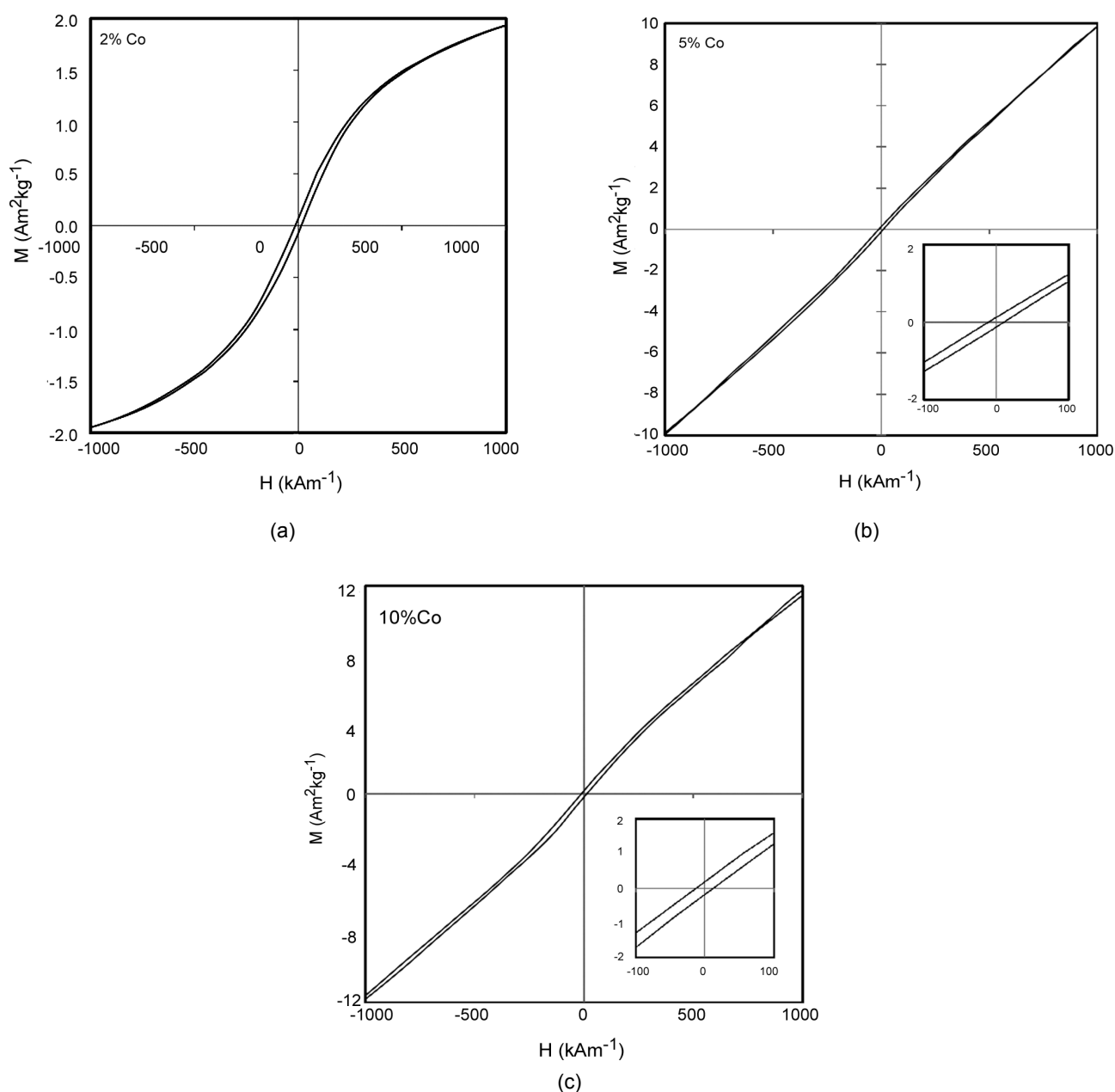| Quality results		Identity results		
Element	line	W%	A%	ZAF
O	Ka	31.18	67.15	0.4966
Co	Ka	1.32	0.77	1.0469
Zn	Ka	57.59	30.35	0.9259
Au	La	9.91	1.73	0.6441
Total	-	100.00	100.00	-

Figure 5: *Hysteresis loops for the samples: a) $Zn_{0.98}Co_{.02}O$, b) $Zn_{0.95}Co_{.05}O$, c) $Zn_{0.90}Co_{010}O$ measured at room temperature.*

greatly suppressed and replaced by paramagnetism at higher Co doping levels (Figure 5b, c).

Interpretation of the ferromagnetism observed in Co-doped ZnO nanocrystals is not easy. It could arise from a number of possible sources: as carrier-mediated exchange mechanism, co precipitation, and the formation of CoO. However, CoO phase can be easily ruled out, since CoO is anti-ferromagnetic with a Neel temperature at 293 K. Second, metallic Co is also an unlikely source of this ferromagnetism, as XRD results clearly show no metallic Co clusters in the prepared samples NPs. UV-visible absorption spectra showed a red band gap shift which suggests Co^+ ions were successfully incorporated into the wurtzite lattice at the Zn^{2+} sites. Thus, ferromagnetism in the Co-

Int. J. Bio-Inorg. Hybd. Nanomat., Vol. 1, No. 2 (2012), 123-130
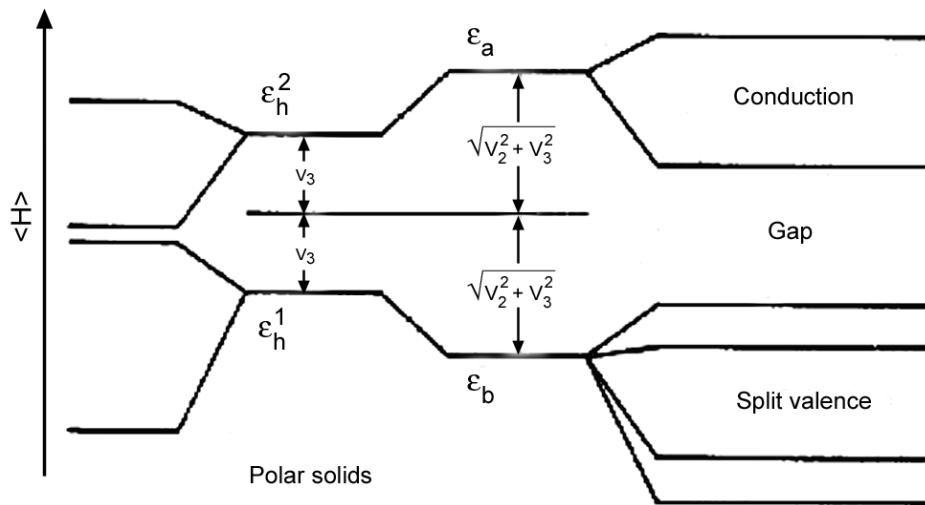
Sadjadi MS et al

Figure 6: *Schematic representation of doping and sp-d exchange interaction Taken from Walter A. Harrison "Electronic Structure and the Properties of Solids-The Physics of Chemical Bond -, 1980.*

doped ZnO NPs could be considered as a result of the exchange interaction between free delocalized carriers (hole or electron) and the localized d spins on the Co^{2+} ions (Figure 6).

3.6. Optical absorption and photoluminescence studies

Figure 7 (a,b,c) shows the optical absorption spectra at room temperature of the pure ZnO, $Zn_{0.98}Co_{.02}O$ and $Zn_{0.998}Co_{.002}O$, displaying absorption bond gap edges at about 370, 380 and 250 nm respectively. These spectra can be used primarily to verify the band gap shift. A red shift can be observed in the band gap energy for the Co-doped samples compared to the undoped ZnO. The red shift is typically attributed to the sp -d exchange between the ZnO band electrons and localized d-electrons associated with the doped Co^{2+} cations. This interaction leads to corrections in the energy bands: the conduction band is lowered and the valence band is raised causing the band gap to decrease [21-22]. Furthermore, three weak absorption peaks were observed at 3.49 (A), 3.75 (B) and 4.00 eV (C) in the Co-doped samples. These peaks can be corresponded to the electronic transition of Co 3d orbital in the oxygen tetrahedron:
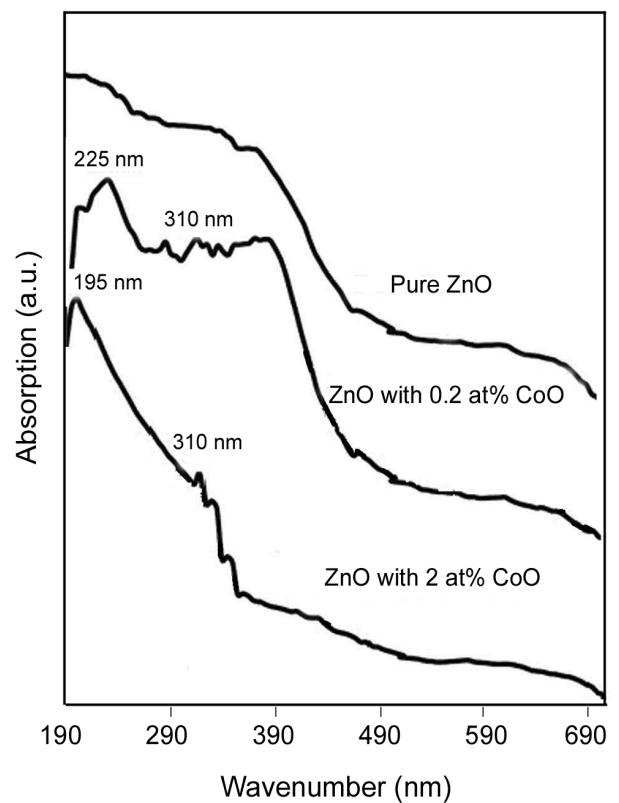

Figure 7: *UV-visible absorption spectrum at room temperature of $Zn_{0.98}Co_{.02}O$, $Zn_{0.998}Co_{.002}O$ in comparison with pure ZnO.*

$^4A_2(F) \rightarrow {}^2E(G)$, $^4A_2(F) \rightarrow {}^4T_1(P)$ and $^4A_2(F) \rightarrow {}^2A_1(G)$, respectively. Similar results have been also reported by others [23, 24]. These results give a further support that the Co^{2+} ions are substituted for the tetrahedrally coordinated Zn^{2+} ions in the nanocrystals.

4. CONCLUSIONS

In this work, to understand the origin of FM in the systems of diluted magnetic semiconductor (DMS), cobalt doped ZnO nanoparticles with different percent of doped cobalt oxide have been successfully synthesized and then, crystallographic and electronic structures of the prepared pure ZnO and the Co^{2+} doped ZnO nanoparticles was investigated. All the diffraction peaks observed in their XRD patterns were contributed to the formation of wurtzite ZnO structure (hexagonal crystal system, P63 mc space group, JCPDS card No. 36-1451). The presence of no other diffraction peaks concerning to the cobalt oxides in the XRD patterns indicates the substitution of Zn^{2+} ions by Co^{2+} ions in the ZnO structure. Appearance of the infrared spectra at 1130 and 1228 cm^{-1} belonging to internal and external asymmetric Zn-O and Co-O stretching modes and the peaks at 458 and 531 cm^{-1} characteristic of the Zn-O and Co-O confirm substitution of Zn^{2+} ions by Co^{2+} ions in the tetrahedral ZnO crystalline structure. Observation of the red shift on the absorption band edge in UV-Vis spectra of cobalt doped ZnO was another indication for sp -d exchange interaction between ZnO bands electrons and well localized d-electrons in the associated ZnO with the doped Co^{2+} cations.

Ferromagnetism behavior measured for cobalt doped ZnO nanoparticles (with 2at% CoO) in the magnetization curve at RT (S- shaped curve in Figure 5a) and its replacement by paramagnetism at the higher Co doping levels (Figure 5b,c) was in conformity with the theory of carrier-mediated exchange, where, low carrier densities of magnetic cobalt ions give rise to a ferromagnetism behavior for the poor conducting ZnO nanoparticles and the high carrier of densities leads to the magnetization

depending on the carrier density. As a conclusion, ferromagnetism in the Co-doped ZnO NPs could be considered as a result of the exchange interaction between free delocalized carriers (hole or electron) and the localized d spins on the Co^{2+}.

REFERENCES

1. Philip J., Punnoose A., Kim B.I., Reddy K.M., Layne S., Holmes J.O., Satpati B., Leclair P.R., Santos T.S., Moodera J.S., *Nature Mater.*, **5**(2006), 298.
2. Sundaresan A., Bhargavi R., Rangarajan N., Siddesh U., Rao C.N.R., *Phys. Rev. B.*, **74**(2006), 161306R.
3. Garcia M.A., Merino J.M., Pinel E.F., Quesada A., Venta J.D., Gonzalez R., Castro G., Crespo P., Liopis J., GonzalezCalbet J.M., Hernando A., *Nano Lett.*, **7**(2007), 1489.
4. Ueda K., Tabata H., Kawai T., *Appl. Phys. Lett.*, **79**(2001), 988.
5. Quesada A., Garcia M.A., Crespo P., Hernando A., *Journal of Magnetism and Magnetic Materials*, **304**(2006), 75-78.
6. Matsumoto Y., Murakami M., Shono T., Hasegawa T., Fukumura T., Kawasaki M., Ahmet P., Chikyow T., Koshihara S., Koinuma H., *Science*, **291**(2001), 854.
7. Sharma P., Gupta A., Rao K.V., Owens F.J., Sharma R., Ahuja R., Osorio J.M., Johansson G.B., Gehring G.A., *Nature Mater.*, **2**(2003), 673.
8. Dietl T., Ohno H., Matsukura F., Cibert J., Ferrand D., *Science*, **287**(2000), 1019.
9. Mofor A., Che El-Shaer A., Bakin A., Waag A., Ahlers H., Siegner U., Sievers S., Albrecht M. et al., *Applied Physics Letters*, **87**(6)(2005), 062501.
10. B. Lin, Z. Fu, Y. Jia, *Appl. Phys. Lett.*, **79**(2001), 943.
11. Garcia M.A., Merino J.M., Pinel E.F., Quesada A., Venta J.D., Gonzalez R., Castro G., Crespo P., Liopis J., Gonzalez- Calbet J.M., Hernando A., *Nano Lett.*, **7**(2007), 1489.
12. Lavat A.E., Wagner C.C., Tasca J.E., *Ceramics*

Int., **34**(2008), 2147-2153.

13. Wu J.J., Liu S.C., Yang M.H., *Appl. Phys. Lett.*, **85**(2004), 1027.

14. Cui J.B., Gibson U.J., *Appl. Phys. Lett.*, **87**(2005), 133108.

15. Yuhas B.D., Zitoun D.O., Pauzauskie P.J., He R., Yang P., *Angew. Chem. Int. Ed.*, **45**(2006), 420.

16. Clavel G., Willinger M.G., Zitoun D., Pinna N., *Adv. Funct. Mater*, **17**(2007), 3159.

17. Wang X., Zheng R., Liu Z., Ho H., Xu J., Ringer S.P., *Nanotechnology*, **19**(2008), 455702.

18. Li J., Fan H., Jia X., Yang W., Fang P., *Appl Phys*. A, **98**(2010), 537-542.

19. Pal B., Giri P.K., *International Journal of Nanoscience*, **10**(1) (2011), 1-5.

20. Pal B., Giri P.K., *J. Nanosci. Nanotechnol*, **11**(2011), 1-8.

21. Li M., Li C.C., Zhang J., Du Z.F., Zou B.S., Yu H.C., Wang Y.G., Wang T.H., *Nanotechnology*, **18**(2007), 225504.

22. Sanon G., Rup R., Mansingh A., *Phys. Rev. B.*, **44**(1991), 5672.

23. Koidl P., *Phys. Rev. B.*, **15**(1977), 2493.

24. Hasuike N., Deguchi R., Katoh H., Kisoda K., Nishio K., Isshiki T., Harima H., *J. Phys. Condens. Matter*, **19**(2007), 365223.